Auger-electron and x-ray production in 50- to 2000-keV Ne+Ne collisions

N. Stolterfoht, D. Schneider, and D. Burch*
Hahn-Meitner-Institut für Kernforschung Berlin GmbH,1 Berlin 39, West Germany

B. Aagaard, E. Bøving, and B. Fastrup
Institute of Physics, University of Aarhus, 8000 Aarhus, Denmark

(Received 12 May 1975)

The production of vacancies in the inner and outer shells of the target and projectile have been studied in $Ne^{i+}+Ne$ collisions in the incident energy range of 45 keV to 2.2 MeV through the observation of K x rays and Auger electrons. Data are given for incident charge states $i=0$, 1, and 2. Parameters necessary for the analysis of collision kinematics were extracted from previous data and used to investigate these effects on the observed Auger spectra. The kinematic line broadening in the Ne collisions is shown to obscure the peak structure characteristic of the multiple ionization states. The centroid energies and average energy widths of the Auger groups, together with absolute intensities, are reported as a function of the Ne^{i+} energy and electron emission angle for both target and projectile. After kinematic corrections, it is found that target and projectile Auger-electron emission are isotropic to within $\pm 10\%$ and that the K vacancy created is equally shared between the target and projectile. The average number $\bar{n}_A$ of electrons removed from the L shell simultaneous with the K vacancy production is estimated from the centroid Auger-electron energies and compared with previously measured data. It is found that $\bar{n}_A$ increases with the Ne^+ energy from ~ 2.5—3.6 over the energy range studied. Absolute cross sections for x-ray and Auger-electron production are reported with an accuracy of about $\pm 15\%$, and mean fluorescence yields are determined from these cross-section data. The fluorescence yield increases with incident Ne^+-ion energy, and is consistent with the observed degree of L-shell ionization. Total K-vacancy production cross sections agree well with available calculations below 200 keV, but the theoretical results underestimate the cross sections at higher energies. This reflects a breakdown of the two-state approximation made in the calculation. Information regarding the coupling of outer-shell molecular orbitals in the entrance channel is extracted from the comparison of the measured data and previous calculations.

I. INTRODUCTION

Inner-shell ionization in slow $Ne^+ + Ne$ collisions has received particular attention in the past few years. Evidence for K-shell ionization has been provided in energy-loss measurements of violent Ne+Ne collisions.[1] The energy-loss experiments have established the basis of the Fano-Lichten model[2-4] which describes inner-shell ionization in terms of electron promotion via molecular orbitals (MO) in a quasimolecule formed during the collisions. In this model, K-shell ionization takes place via vacancy transfer from the $2p\pi$ MO to the $2p\sigma$ MO by a rotational coupling mechanism. As pointed out by Lichten,[3] the K-shell ionization cross section is expected to be proportional to the number of $2p\pi$ vacancies present before the collision. This "exit channel" effect has partly been confirmed by McCaughey *et al.*,[5] who have found in Auger-electron measurements that the ratios of K-shell ionization probabilities are 2:1:0.6 for 200-keV Ne^{2+}, Ne^+, and Ne^0 impact on Ne. The unexpected high ionization probability for Ne^0 impact clearly showed the need for further studies.

Using the technique of Auger-electron spectroscopy,[6] Cacak *et al.*[7] have determined total cross sections for K-shell excitation in 50- to 300-keV $Ne^+ + Ne$ collisions. These results[7] are in good agreement with calculations by Briggs and Macek,[8] who deduced cross sections for Ne K ionization on the basis of the Fano-Lichten model. The calculations yielded probabilities for transitions by rotational coupling of the $2p\pi$ and $2p\sigma$ MO's. Experimental information about the $2p\pi$-$2p\sigma$ transition probabilities have been achieved in x-ray–ion coincidence experiments by Sackmann *et al.*[9] and in energy-loss measurements by Fastrup *et al.*,[10] who have also found a 2:1 ratio for Ne^{2+} and Ne^+ impact ionization probabilities. Recently, using Auger-electron spectroscopy, Fastrup *et al.*[11] have shown that the Ne^{2+}-Ne^+ cross-section ratio is dependent on the projectile velocity. These measurements indicate that, in the incoming part of the collision, additional $2p\pi$ vacancies are produced with increasing probability as the collision energy increases.

Apart from the possibility of obtaining total ionization cross sections, Auger-electron spectra generally yield further information. The spectra are affected by collision kinematics; when observed at specific observation angles, the peaks of Auger electrons from the projectile and the target atom are clearly separated for Ne+Ne due

to the kinematic (Doppler) shift of the projectile Auger peak. The peak separation allows for a separate study of Auger-electron ejection from projectile and target atoms. Thus, the K-shell vacancy sharing between the two collision partners can be deduced. Previously, inner-shell vacancy sharing has been studied primarily in asymmetric collisions.[12,13] Furthermore, the degree of outer-shell ionization produced in the K-shell ionization collision can be estimated from the energy distribution of the Auger electrons from both particles. In the past, only a few Auger spectra have been reported from Ne+Ne collisions. Kessel *et al.*[14] have measured a first spectrum of Auger electrons from both the Ne projectile and the target atom. Auger spectra for 100-, 200-, and 400-keV Ne^+ impact on Ne have been analyzed by Stolterfoht *et al.*[15] using a different spectrometer than applied in this work.

Cross sections for x-ray production in Ne^++Ne collisions have been reported[16-19] for the projectile energy range of 20–1200 keV. Saris and Onderdelinden[16] have combined their x-ray results for 50- and 100-keV Ne^+ with cross sections for Auger production by Cacak *et al.*[7] to determine Ne K fluorescence yields averaged over multiple ionization states. A similar comparison in the extended energy range of 50–200 keV has been carried out by Tawara *et al.*,[17] who also used Ne^{2+} projectiles. This analysis was made to study a possible variation of the Ne K fluorescence yield with projectile energy. Larkins[20] and Bhalla *et al.*[21] had previously shown theoretically that the mean fluorescence yield is sensitively dependent on the Ne outer-shell configuration produced in the collision. However, it should be noted that Tawara *et al.*[17] quoted considerable uncertainties in the fluorescence yield deduced by comparison of results from different laboratories. Instrumental uncertainties can be reduced when x rays and Auger electrons are simultaneously measured in one apparatus as done by Burch *et al.*[22] for 30-MeV O^{5+}+Ne. Recently, high-resolution x-ray measurements have also been made by Matthews *et al.*[19] for 100–1000-keV Ne^++Ne. Related studies of the fluorescence yield of Ne have been reported in Refs. 23–26.

In the present work, experimental results from laboratories at the University of Aarhus and the Hahn-Meitner-Institute at Berlin are combined for a comprehensive study of x-ray and Auger-electron production in Ne+Ne collisions. At Aarhus, Auger electrons were observed at an angle of 96.6° with respect to the incident beam to deduce K-shell ionization cross sections for 45- to 2250-keV Ne impact. Measurements were made with Ne^{2+}, Ne^+, and Ne^0 impact to study the "exit-channel" effect. Furthermore, to obtain fluorescence yields, the present results can be compared with the x-ray data given by Schartner *et al.*[18] At Berlin, Auger-electron spectra for 50- to 600-keV Ne^++Ne were measured at 30°, 90°, and 150° to study angular distribution in the ejection of Auger electrons, K-shell vacancy sharing in projectile and target atom, and multiple ionization effects. Moreover, cross sections for production of x rays and Auger electrons were measured simultaneously in one apparatus to reduce uncertainties in the determination of the fluorescence yield.[27]

In Sec. II, instrumental details are given. Collision kinematics are analyzed in Sec. III. In Sec. IV, experimental results are presented and discussed. Conclusions from the results are given in Sec. V.

II. EXPERIMENTAL

The apparatus (A) used in the laboratory at Aarhus has been described elsewhere.[28] Incident ions were charge analyzed by a bending magnet and subsequently monitored in a Faraday cup. Neutral beams were produced in a charge exchange chamber followed by an electrostatic deflection system used to remove remaining ions. The neutral beam was detected by a monitor which incorporates a Faraday cup and an extraction electrode to measure the current of secondary electrons produced in the cup. The monitor system for neutral atoms was calibrated by a Ne^+ beam of known intensity. The pressure in the target cell was measured by a calibrated Pirani gauge to within a few percent. The target gas pressure was $\sim 5\times10^{-4}$ Torr over a length of ~3 cm, and it was maintained sufficiently low to prevent the incident beam from charge-exchange collisions. Electrons ejected at 96.6°±3° with respect to the incident beam direction were analyzed by a spherical electrostatic spectrometer with an energy resolution of either 1.5% or 4.0% full width at half-maximum (FWHM). The electron detector was a Mullard channel electron multiplier of type B419BL. The combined analyzer plus detector efficiency was determined to be 0.66 by comparing 50-keV Ar+Ar L-MM Auger yields with corresponding yields obtained by Cacak *et al.*[7] at 90° emission angle. The absolute value of Cacak *et al.*[7] for the total L-MM Auger cross section integrated over all emission angles, which is 3.30×10^{-17} cm^2, agrees well with an $L_{2,3}$ ionization cross section derived from inelastic energy-loss measurements.[29] In the latter case, an integration over $d\sigma_{L_{2,3}} = 2\pi\alpha(R_0)b\,db$, where $\alpha(R_0)$ is the $L_{2,3}$ electron-promotion probability, R_0 is the distance of closest approach in the collision, and b is the impact

parameter, yields the result $\sigma_L = 3.24\times10^{-17}$ cm^2. After having determined the detector efficiency, absolute cross sections for Auger-electron production could be deduced.

The apparatus (B) used in the laboratory at Berlin for Auger-electron measurements has also been described in detail previously.[30,31] In this work, an x-ray detector was incorporated in the apparatus. The collimated incident ion beam was crossed by an atomic neon beam ejected from a nozzle in the center of the chamber. The product of the gas target density and thickness was ~5 $\times10^{-3}$ Torr$\times$3 mm. It was sufficiently small so that single-collision conditions were provided in the experiments. Pressure measurements were made using an ionization gauge calibrated by a capacitance manometer. Electrons produced in the collision region were measured by a parallel-plate electrostatic spectrometer. The resolution was generally 2.6% FWHM. In specific cases the resolution was improved by decelerating the incident electrons as described previously.[31] The electron observation angle could be varied continuously from 22° to 152°; in the present study, measurements were made at 30°, 90°, and 150°. Angular acceptance of the analyzer is ±3°. The analyzer efficiency was calibrated by an electron source of known emission per solid angle. X rays were measured by a technique similar to that used by Saris and Onderdelinden.[16] A flow-mode proportional counter with a 2-μm Makrofol window foil detected x rays at 90°. The transmission of (41±3)% for the detector-window foil was determined by using a second foil temporarily placed in front of the detector window. The window transmission was found to be independent of the Ne-beam energy. The solid angle of 1.48×10^{-3} sr and the viewed beam length of 12 mm were determined from the slit geometries. The measured Ne K x-ray spectrum consisted of a well-defined single peak with essentially no background. Absolute cross sections for production of x rays and Auger electrons were measured using a well-known homogeneous pressure in the gas-target region. These results were used to normalize the data obtained with the atomic beam, whose density was not known exactly.[30]

III. COLLISION KINEMATICS

In the laboratory frame, we consider a particle of energy T_0 incident on a target atom at rest. Let T_1 and β_1 be, respectively, the energy and the scattering angle of the projectile after the collision. T_2 and β_2 are the corresponding quantities for the recoiling target atom. For a given T_0 and inelastic energy loss Q, it follows from energy and momentum conservation that the values of β_1, β_2, T_1, and T_2 can be determined if any one of these four quantities is known. The deduction of one of these quantities, none of which is determined in the present measurements, needs a model calculation including information about the specific excitation process.

The differential scattering cross section $d\sigma(\beta_1)/d\Omega$ was folded with the β_1-dependent probability P_{II} for $2p\sigma$-$2p\pi$ transitions as measured by Fastrup *et al.*[10] for 200-keV Ne^++Ne, i.e.,

$$f(\beta_1) = P_{II}(\beta_1) 2\pi \sin\beta_1 \frac{d\sigma(\beta_1)}{d\Omega} .$$

It was found that the distribution $f(\beta_1)$ has a maximum at 10° and a FWHM of 6°. In the following, $\overline{\beta}_1$ denotes this centroid value and $\Delta\beta_1$ the width of the maximum. The projectile is scattered in a cone symmetric with respect to the incident-beam direction. For 200-keV Ne+Ne, the product of the cone angle of 10° and the impact energy is $\overline{\beta}_1 T_0 = 2000$ keV deg. Since this product is found to be nearly constant in a K-shell ionization collision,[1] values of $\overline{\beta}_1$ could be derived for impact energies other than 200 keV. The centroid values $\overline{\beta}_2$, $\overline{T}_1$, and $\overline{T}_2$ were then calculated from the collision kinematics with $Q = 1360$ eV.[10] The results partly shown in Table I indicate that, generally, a rather large recoil energy is transferred to the target atom. Hence, Auger spectra from both projectile and recoil atom are expected to be influenced by kinematic effects.

We consider now the intensities I and I' per sr of Auger lines in the laboratory system and in the rest frame of the emitter particle, respectively. Let $d\Omega$ and $d\Omega'$ be the corresponding solid angles. A simple analysis based on $I/I' = d\Omega'/d\Omega$ yields for the electron observation angle θ,

$$\frac{I}{I'} = \frac{E}{E'}\left(1 - \frac{t}{E'}\sin^2(\theta-\beta)\right)^{-1/2} \approx \frac{E}{E'} , \qquad (1)$$

TABLE I. Scattering angle $\overline{\beta}_1$ and energy $\overline{T}_1$ of projectiles producing K-shell ionization in Ne+Ne collisions. $\overline{\beta}_2$ and $\overline{T}_2$ are the corresponding quantities for the target recoil atom. T_0 is the incident energy. The angle $\overline{\beta}_1$ was obtained from $T_0\overline{\beta}_1 = 2000$ keV deg.

T_0 (keV)	$\overline{\beta}_1$ (deg)	$\overline{\beta}_2$ (deg)	$\overline{T}_1$ (keV)	$\overline{T}_2$ (keV)
50	40	48	28	21
70	29	60	52	16
100	20	69	87	11.7
200	10	79	192	6.0
500	4.0	85	496	2.4
1000	2.0	86.8	997	1.2
2000	1.0	87.8	1998	0.6

where E and E' are the energies of the Auger line in the lab system and the particle frame, respectively, and β is the cone angle of the emitter particle. The reduced energy $t = T/\lambda$ follows from the energy T of the emitter particle and the ion mass λ in emu. The approximation $I/I' \approx E/E'$ is valid for $t \ll E'$, which is fulfilled in the present analysis.

The rest-frame energy of a kinematically shifted Auger line is[6]

$$E' = E - 2(Et)^{1/2}\cos\theta\cos\beta + t \ . \tag{2}$$

There are different effects which cause Auger-line broadening in ion-atom collisions. Broadening of (base) width ΔB_c occurs since the emitter particles are scattered into a cone rather than at one definite azimuthal angle. Additional broadenings ΔB_β, ΔB_Q, and ΔB_θ are present when β, Q, and θ vary within the intervals $\Delta\beta$, ΔQ, and $\Delta\theta$, respectively. Assuming the angular spread in the incident-ion beam is completely negligible, relations for broadening effects can be summarized as follows:

$$\Delta B_c = 4(Et)^{1/2}\sin\theta\sin\beta \ , \tag{3a}$$

$$\Delta B_\beta = \Delta\beta F(\beta), \tag{3b}$$

$$\Delta B_Q = \Delta Q\, G(Q) \ , \tag{3c}$$

$$\Delta B_\theta = \Delta\theta 2(Et)^{1/2}\sin\theta\cos\beta \ . \tag{3d}$$

The (approximate) relation (3a) has been derived by Rudd and Macek.[6] (A slightly incorrect formula has previously been given by Ogurtsov *et al.*[32]) Formulas (3b)–(3d) are deduced from Eq. (2) by differentiation with respect to β, Q, or θ. Thus, it follows that $F(\beta) = dE'/d\beta$, and $G(Q) = dE'/dQ$, where E' is given by Eq. (2) and expressions for collision kinematics. It should be noted that line broadening corresponding to Eqs. (3a)–(3c) follows from collision kinematics, whereas Eq. (3d) describes an instrumental effect caused by the finite acceptance angle of the electron analyzer. Furthermore, it should be emphasized that Eqs. (1) and (3) apply only to monoenergetic Auger lines or to a group of sufficiently small width.

As an example, the broadening of Auger lines is estimated for 50-, 500-, and 1500-keV Ne impact on Ne. In the calculations, the centroid values $\bar{t}_1 = \bar{T}_1/\lambda$ and $\bar{\beta}_1$ for the projectile and $\bar{t}_2 = \bar{T}_2/\lambda$ and $\bar{\beta}_2$ for the recoil atom are inserted in Eqs. (3a)–(3d) for t and β, respectively. The analyzer acceptance angle is $\Delta\theta = 6°$, as mentioned above. The numbers of $\Delta\beta_1$ and, consequently, those of $\Delta\beta_2$ for 50-, 500-, and 1500-keV Ne+Ne are estimated from the FWHM $\Delta\beta_1 = 6°$ for 200-keV Ne+Ne under the assumption that $\bar{\beta}_1 T_0 = \text{const}$. Results are given in Table II for the electron observation angles of $\theta = 30°$, 90°, and 96.6°. (The results for 150° are similar to those of 30°.) It is seen that ΔB_c and ΔB_β decrease with increasing projectile energy. This behavior is typical for broadening produced by kinematic effects. For angles of $\theta = 30°$, 90°, and 150° studied in this work, ΔB_c dominates. However, for 0° and 180°, the contribution of ΔB_β is largest. Thus, the broadening effects cannot be completely avoided by choosing specific electron observation angles such as 0° or 180°. Furthermore, it is seen that the values of ΔB_c and ΔB_β for the projectile are nearly equal for the corresponding quantities of the recoil atom. This follows from the fact that the velocity components perpendicular to the incident beam are equal for the scattered projectile and the recoil atom, i.e., $\bar{t}_1^{1/2}\sin\bar{\beta}_1 = \bar{t}_2^{1/2}\sin\bar{\beta}_2$. In contrast to the behavior of ΔB_c and ΔB_β, the broadening ΔB_θ caused by the finite acceptance angle of the electron analyzer increases with increasing collision energy, and it is relevant only for the projectile. It is expected that the contribution of ΔB_θ plays the dominant role in the projectile energy region of several MeV.

IV. RESULTS AND DISCUSSION

A. Auger spectra

To obtain a general picture of Auger-electron production in collisions of heavy ions on Ne, a comparison is made in Fig. 1 for Auger spectra of Ne excited by different projectiles.[23,33,34] Figure 1 shows primarily Auger electrons from the target; for Ne+Ne, the projectile Auger peak is kinematically shifted outside the plotted energy range. The Ne+Ne spectrum was measured with relatively high resolution so that the shape of the

TABLE II. Widths ΔB_c, ΔB_β, and ΔB_θ of line broadening of Auger peaks observed at angle θ. Labels (P) and (T) denote the projectile and the target atom. The incident Ne energy is T_0.

T_0 (keV)	Particle	θ (deg)	ΔB_c (eV)	ΔB_β (eV)	ΔB_θ (eV)
50	(P)	30	32	19	2.5
		90	64	0	4.8
	(T)	30	31	18	1.1
		90	62	0	2.2
500	(P)	30	16	0.7	12
		90	28	0	20
	(T)	30	14	0.6	0.06
		90	28	0	0.12
1500	(P)	96.6	16	0	34.5
	(T)	96.6	15	0	0.04

plotted spectrum is not influenced by the limited resolution. The prominent feature of the spectra in Fig. 1 is the variation of the centroid Auger energy. For the cases shown, the recoil energy transfered to the Ne target is sufficiently small that kinematic energy shifts can be neglected. The Auger peaks are shifted to lower energies because outer-shell vacancies are produced in addition to the inner-shell vacancy. The average numbers of L-shell vacancies are 0.23, 2.8, 2.9 and ~6 for 4.2-MeV H^+, 500-keV Ne^+, 30-MeV O^+, and 50-MeV Cl^{15+} impact, respectively (see below and Refs. 23, 26, and 34). These numbers show that 500-keV Ne^+ and 30-MeV O^{5+} produce nearly the same number of L-shell vacancies, as indicated by the centroid energies of the corresponding peaks, which nearly coincide in energy. However, there are considerable differences in the structures of the two peaks. The 30-MeV O^{5+}+Ne spectrum shows a large number of distinct lines (see also Ref. 35), whereas the 500-keV Ne^++Ne spectrum appears as a broad maximum. This observation is explained by kinematic line broadening which is relatively large for slow Ne impact. The numbers in Table II show that for 500-keV Ne+Ne, the line broadening of ~20 eV is much larger than the typical line separation of ~3 eV. Therefore, individual lines cannot be seen, although the resolution of 2.6-eV FWHM is rather small. This shows that improved resolution does not supply additional information in the case of low-energy Ne+Ne collisions. Thus, in this work, most Auger spectra were measured with relatively low resolution of 15- to 30-eV FWHM.

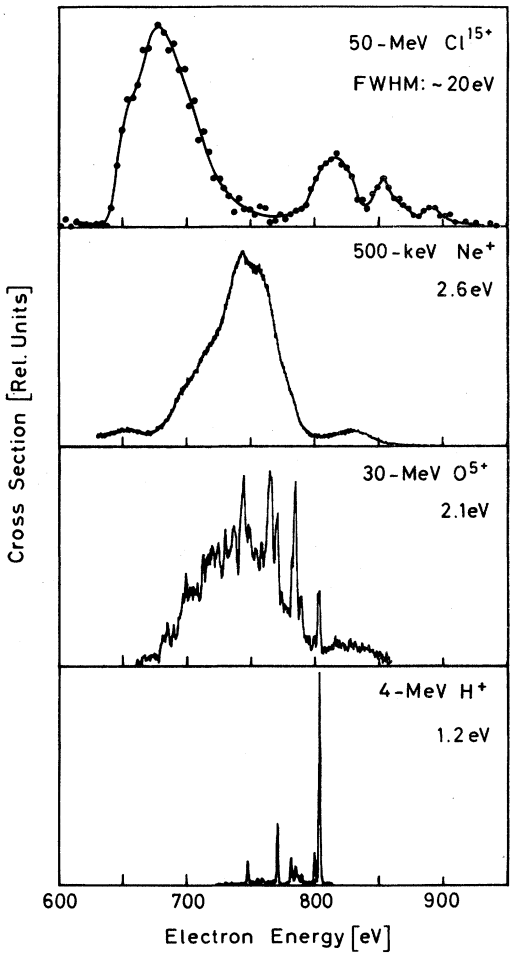

FIG. 1. Ne K Auger spectra observed at 150° in various ion-atom collisions. The 500-keV Ne^+ + Ne spectrum is from Berlin. The 50-MeV Cl^{15+} + Ne, 30-MeV O^{5+} + Ne, and 4.2-MeV H^+ + Ne data are taken from Refs. 23, 33, and 34, respectively. Energy resolutions (FWHM) are ~20, 2.6, 2.1, and 1.2 eV, as indicated. Continuous electron backgrounds are subtracted. The 500-keV Ne + Ne spectrum shows electrons primarily from the target; electrons at energies below ~660 eV originate from the projectile.

Apart from the main peak at 748 eV, the Ne+Ne spectrum shows a smaller peak at 827 eV. A similar peak is present in the O+Ne spectrum, and for Cl+Ne, additional structures appear at even higher energies. It should be noted that these peaks are higher in energy than the normal lines seen in the H+Ne spectrum. Auger electrons of such high energies may be ejected when the Ne atom is doubly ionized in the K shell[21] or when electrons excited to upper bound states participate in the Auger transition.[36] Auger peaks resulting from double K-shell ionization are expected to be shifted to lower energies as additional vacancies are produced in the outer shells.[21] However, Fig. 1 shows that the high-energy peak is hardly shifted as different projectiles are used. This finding supports the assumption that excitation to upper bound states plays the dominant role in the present case. For Cl+Ne, it is very likely that the high-energy peaks are due to electron ejection from multiply excited Li- and He-like Ne.

In Figs. 2 and 3 are plotted Ne+Ne spectra produced by projectiles of different charge states and observed at different angles. The curves show Auger peaks from the target atom and kinematically shifted peaks from the projectile which are labeled by P and T, respectively. The kinematic energy shifts decrease with decreasing projectile energy. This produces an increasing overlap of the projectile and target peak. However, it was found that the shape of the Auger peak does not substantially change as the energy of the incident ion is varied. Thus, the spectra could be unfolded, fitting each peak by a generalized curve with position, height, and width as variable parameters.[15]

B. Outer-shell ionization

To study the Auger spectra we consider the intensity I_j', the centroid energy $\bar{E}_j'$, and the FWHM $\Delta W_j'$ for the Auger peaks from the projectile ($j=1$) and target ($j=2$) in the rest frame of the corresponding particles; I_j, $\bar{E}_j$, and ΔW_j are the related quantities in the laboratory system. These values were obtained by unfolding the Auger spectra. Some results are given in Table III for observation angles of 30° and 150°. Integration of the spectra observed at 90° or 96.6° yields the sum $2I_{1,2}=I_1+I_2$. In Table III the value $I_{1,2}(90°)$ was used to normalize I_1 and I_2 for a given T_0. Uncertainties in $I_j/I_{1,2}$ are typically ±10%. Uncertainties in the ratio of I_1 and I_2 for a given angle are generally smaller than ±10% since these numbers were obtained from one spectrum. Uncertainties of ±3 and ±4 eV were estimated for the fitted energy $\bar{E}_j$ and width ΔW_j, respectively.

Using Eq. (2), the rest-frame energy $\bar{E}_j'$ was derived from $\bar{E}_j$, and is shown in Fig. 4(a). Recalling that the energy $\bar{E}_j'$ is a measure for the degree of outer-shell ionization, we can summarize the data as follows:

(a) Rest-frame energies of the Auger peaks observed at 30° and 150° are equal within the experi-

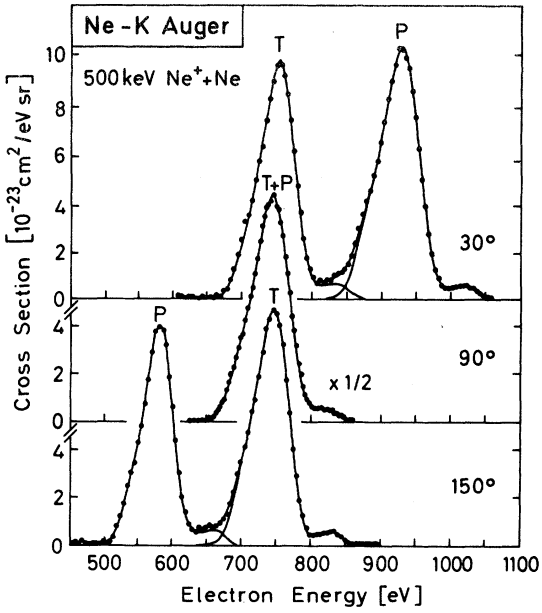

FIG. 2. Double differential cross sections for production of Ne K Auger electrons in 500-keV Ne^+ + Ne collisions. Data are from Berlin. Electron observation angles are 30°, 90°, and 150°, as indicated. Continuous electron background is subtracted. Auger peaks from the projectile and the target are labeled by P and T, respectively. Energy resolution (FWHM) is 2.6%.

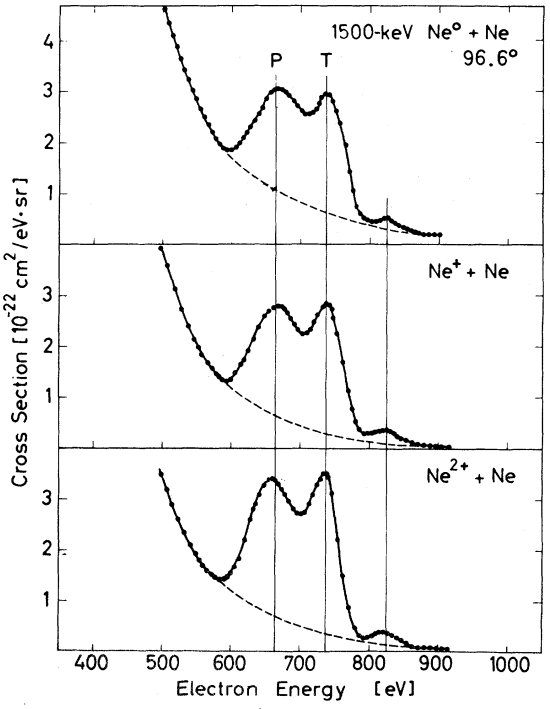

FIG. 3. Double differential cross section for Auger-electron production by 1.5-MeV Ne^0, Ne^+, and Ne^{2+} incident on Ne. Data are from Aarhus. Observation angle is 96.6°. Peaks from the projectile and the target are labeled by P and T, respectively. Energy resolution (FWHM) is 4%.

TABLE III. Intensity I_j, centroid energy $\bar{E}_j$, and FWHM ΔW_j of the projectile ($j=1$) and target ($j=2$) Auger peaks observed at laboratory angle θ. The incident projectile energy is T_0. The intensity I_j is normalized by $I_{1,2}=[I_1(90°)+I_2(90°)]/2$.

T_0 (keV)	θ (deg)	$\frac{I_1}{I_{1,2}}$	$\frac{I_2}{I_{1,2}}$	$\bar{E}_1$ (eV)	$\bar{E}_2$ (eV)	ΔW_1 (eV)	ΔW_2 (eV)
60	30	1.00	0.96	797	769	76	72
	150	0.93	0.98	710	729	68	73
70	30	1.04	1.01	797	766	74	70
	150	0.98	1.01	705	732	72	77
100	30	0.92	0.99	816	762	75	70
	150	0.89	0.89	686	738	69	73
200	30	1.08	0.99	860	757	70	67
	150	0.85	0.95	646	744	61	70
400	30	1.08	0.95	907	751	68	59
	150	0.80	0.97	599	748	53	61
600	30	1.18	1.00	944	748	70	60
	150	0.87	1.06	568	747	54	58

mental uncertainties, as expected. This finding confirms the results of Table I for kinematic parameters used to convert the laboratory energies into the rest-frame energies. Alternatively, if the kinematic parameters are not known, measurements of Auger energies can be used to derive these parameters, such as projectile scattering angle or recoil energy. These quantities can further be used to obtain information about the scattering potential.

(b) Auger-energy shifts are only slightly different when Ne^{2+}, Ne^{+}, or Ne^{0} are used as projectiles. This shows that the number of outer-shell vacancies produced in the collision is only weakly dependent of the incident charge state.

(c) The centroid energy of the Auger peaks from the projectile and the target are equal in the energy range of 60–600 keV, indicating that the incident charge-state difference is not preserved in the collision. The projectile Auger peak observed in the range of 600–2000 keV suggests that the energy $\bar{E}_1'$ [not plotted in Fig. 4(a)] is slightly lower than the corresponding $\bar{E}_2'$ of the target; this difference increases with increasing incident energy. Although the uncertainty of the centroid energy does not allow a definite conclusion, the data give some indication that the incident charge state difference is slightly preserved in high-energy collisions. This might be expected when the quasimolecular model of the collision breaks down. Recently, Stolterfoht *et al.*[37] have shown, for 30-MeV $O^{4+}+O_2$ collisions, that the post-collision charge state of the projectile is considerably higher than that of the target.

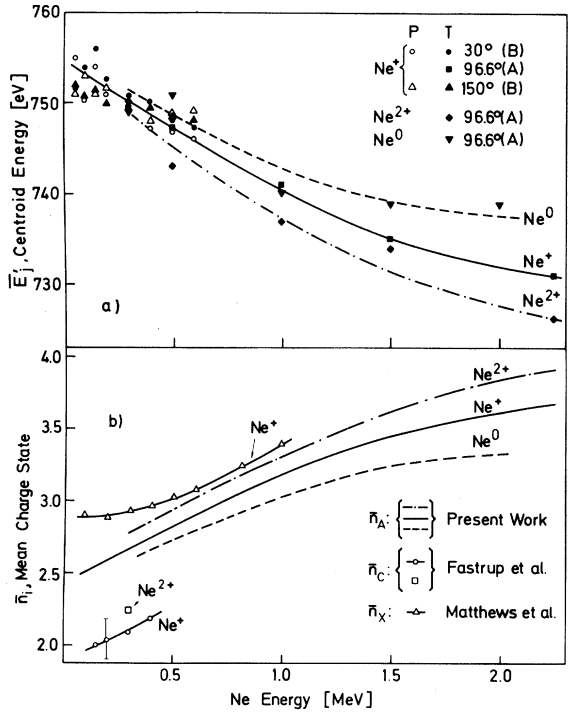

FIG. 4. Centroid energy of Auger peaks and mean outer-shell charge state as a function of the energy of Ne^{0}, Ne^{+}, and Ne^{2+} incident on Ne. (a) Centroid energy $\bar{E}_j'$ of an Auger electron ejected in the rest frame of the corresponding emitter particles. Labels P and T denote the projectile and the target, respectively. Laboratory observation angles are 30°, 90°, 96.6°, and 150°, as indicated. Labels A and B denote apparatus used at Aarhus and Berlin, respectively. (b) The average number $\bar{n}_i$ ($i = X, A$, and C) of outer-shell vacancies simultaneously produced with a K-shell vacancy in the projectile or target atom. $\bar{n}_A$ is derived from the Auger centroid energies $\bar{E}_j'$, $\bar{n}_X$ is obtained from x-ray spectra in Ref. 19, and $\bar{n}_C$ is derived in the Appendix using data from Ref. 10 (see text).

(d) The centroid energy $\bar{E}_j'$ decreases as the Ne energy increases, indicating that the degree of outer-shell ionization varies noticeably in the studied energy range.

The centroid energy of the Auger spectra can be used to estimate the degree of outer-shell ionization before the Auger transition. To do this, we denote the mean number of electrons removed from the L shell as $\bar{n}_A$, where the index A refers to the method of Auger-electron spectroscopy used to estimate the degree of L-shell ionization. (Below we shall see that there are other methods for making this analysis which treat electrons excited to upper bound states differently.) Assuming a one-to-one correspondence between $\bar{n}_A$ and the Auger centroid energy $\bar{E}_j'$, one can draw a smooth curve through the data points given by $\bar{n}_A = 0.23$, 2.9, and ~6 vs $\bar{E}_j' = 791$, 746, and 677 eV for 4-MeV H^{+}, 50-MeV O^{5+}, and 50-MeV Cl^{15+} incident on Ne, respectively (see Fig. 1). From this correspondence and the data for $\bar{E}_j'$ given in Fig. 4(a), the charge-state values were estimated as plotted in Fig. 4(b). (It was found that the uncertainty of $\bar{n}_A$ for Cl+Ne is not significant for the present analysis.) The curves show that $\bar{n}_A$ increases from 2.5 to 3.6 as the Ne^{+} energy increases from 0.1 to 2 MeV. Moreover, slightly higher and lower $\bar{n}_A$ are produced by Ne^{2+} and Ne^{0}, respectively.

In Fig. 4(b), the $\bar{n}_A$ are compared with experimental results as obtained using different methods. $\bar{n}_C$ is the mean number of outer-shell vacancies as obtained from the charge-state and energy-loss measurements by Fastrup *et al.*[10] (see the Appendix). We note that $\bar{n}_C$ represents the mean number of electrons removed into the continuum, i.e., electrons excited to upper bound states are not taken into account. In Fig. 4(b), $\bar{n}_X$ are obtained from high-resolution x-ray measurements.[19] Transition energies of x rays are primarily sensitive to electrons missing from the L shell, regardless

of whether they are removed to bound states or the continuum. Thus, in the case of x-ray spectroscopy, electrons excited to bound states can approximately be treated as if they have been removed to the continuum. The difference in $\bar{n}_C$ and $\bar{n}_X$ might reflect the mean number of electrons excited to bound states.[19] The data for $\bar{n}_A$ are based primarily on $\bar{n}_A = 2.9$ for 30-MeV O^{5+}+Ne, which is supposed[26] to represent the mean number of L-shell vacancies as $\bar{n}_X$ does. The discrepancies between $\bar{n}_A$ and $\bar{n}_X$ are within the uncertainties of the two methods used for the analysis.

C. Electron angular distribution and K-vacancy sharing

First, a few remarks about the width of the Auger peaks are in order. There are several broadening effects present in Ne+Ne collisions. This broadening produces widths of ~20 to ~40 eV in spectra observed at 30° (or 150°) for 50- to 500-keV Ne+Ne, respectively, whereas the total width of a Ne+Ne Auger group is ~60 eV. Thus, assuming the widths to add in quadrature, it is not expected that the broadening effects considerably influence the *over-all* shape of the spectra. In particular, the difference in the widths of 54 and 70 eV for Auger spectra observed at 30° and 150°, respectively, for 600-keV Ne+Ne, is not understood in terms of the broadening effects described by Eqs. (3). This difference must be explained by a transformation of the frame of reference. For a given incident energy, the widths $\Delta W_j'$ of Auger peaks observed in the rest frame of the emitter particles are actually found to be equal within the experimental uncertainties as seen in Fig. 5. Transformation into the laboratory system

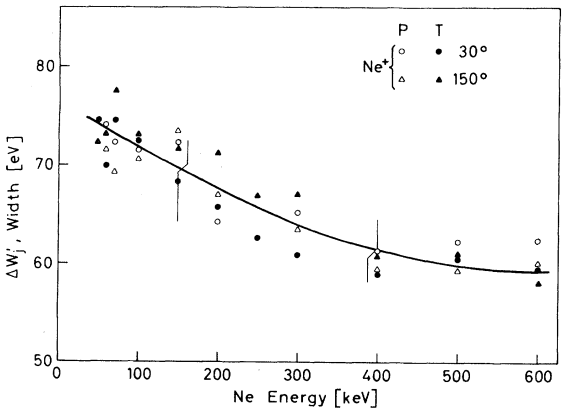

FIG. 5. Width $\Delta W_j'$ of Auger peaks from the projectile (P) and the target (T) as a function of the energy of Ne^+ incident on Ne. Data are from Berlin. $\Delta W_j'$ refers to the rest frame of the corresponding emitter particle. Laboratory observation angles are 30° and 150°, as indicated.

"stretches" or "compresses" the Auger peaks as they are shifted to lower or higher energies, respectively. It should be noted that broadening effects according to Eqs. (3) do wash out spectral structures, whereas "stretching" leaves intrinsic structures unchanged. Figure 5 shows that for the total width of the Auger groups, broadening effects are significant only at low incident energies. Here, the magnitude of $\Delta W_j'$ is equal to that which one would expect from the total Auger group width and the kinematical width added in quadrature.

It has often been assumed that emission of K-LL Auger electrons is isotropic in ion-atom collisions.[6] In principle, this might not be true for initial states with angular momentum $J > \frac{1}{2}$, as shown previously for Ar L_3-shell excitation.[38] In the case of K-shell ionization, the initial angular momentum is $J = \frac{1}{2}$, if the outer shell remains undisturbed in the collision. However, because of the strong outer-shell ionization in Ne+Ne collisions, it is certain that some initial states with $J > \frac{1}{2}$ are produced, and consequently, Auger-electron emission might not be isotropic. The angular distribution of Auger electrons is generally described[38] by $a + b\cos^2\theta$, where a and b are constants, so that the (rest-frame) intensities of the Auger peaks are equal for a pair of observation angles symmetric to 90°, and a possible anisotropy can be studied by comparing $I_j'(30°)$ or $I_j'(150°)$ with $I_j'(90°)$. In the following we use the average value $I_j'(30°, 150°) = \frac{1}{2}[I_j'(30°) + I_j'(150°)]$ to reduce experimental uncertainties. With the centroid energies $\bar{E}_j$ from Table III, it can be shown by means of Eq. (1) that kinematic effects nearly cancel as intensities are summed for a symmetric pair of angles, i.e., $I_j'(30°) + I_j'(150°) \approx I_j(30°) + I_j(150°)$. (This approximation is accurate to within 1% for the cases studied here.) It follows that $I_j'(30°, 150°)/I_j'(90°) = [I_j(30°) + I_j(150°)]/[I_1(90°) + I_2(90°)]$, where we used $I_j'(90°) \approx I_j(90°)$ [see Eq. (1)], and $I_1'(90°) = I_2'(90°)$ as shown below. Figure 6(a) indicates that $I_j'(30°, 150°)/I_j'(90°)$ is 1.0 within experimental uncertainties. This demonstrates the isotropic Auger emission from both the projectile and the target atom in the studied energy range.

Recently, vacancy sharing between projectile and target atoms has been studied in asymmetric collisions.[12,13] Meyerhof[12] has suggested that the sharing deviates strongly from unity as the energy separation of the $2p\sigma$ and $1s\sigma$ MO's increases at large internuclear distances r. For Ne+Ne, the $2p\sigma$ and $1s\sigma$ MO's are degenerate at large r. This degeneracy may be removed if the precollision charge-state difference is preserved during the collision.[39] In this case, K-shell vacancies may not be equally shared between Ne projectile and

target atom. The preservation of the precollision charge-state difference and the nonequal vacancy sharing has previously been observed in 30-MeV $O^{4+}+O_2$ collisions.[37] A possible nonequal vacancy sharing can be studied by comparing the Auger intensities I_1' and I_2'. In Fig. 6(b), the ratio $I_1'(30°,150°)/I_2'(30°,150°)$ is plotted. The data show that the sharing ratio is 1.0 within the experimental uncertainties, indicating that for 50–500 keV, the K-shell vacancies are equally distributed in projectile and target atom. This result is consistent with the observation that the post-collision charge states of projectile and recoil atom are equal.

D. Total cross sections

Total cross sections for production of x rays and Auger electrons were derived by numerical integration of the corresponding spectra. Both x rays and Auger electrons were assumed to be emitted isotropically. Before integration, the spectra were corrected for background and the anisotropy induced by the kinematics of the collision. The background in the spectra was determined by fitting a second-order polynomial to the logarithm of the spectral intensities in the regions of the x-ray or Auger-electron peaks.[31]

In Table IV are given the total cross sections σ_A^i and σ_X^i for production of Auger electrons and x rays by Ne^{i+} impact with $i=0$, 1, and 2. The error in the absolute cross sections is ±15%, which is primarily caused by uncertainties in the determination of the target gas pressure and the detector efficiency. The relative uncertainty in the cross sections with respect to the variation of the projectile energy or charge state is typically ±10% due to counting statistics, beam integration, and background subtraction. In Figs. 7 and 8, σ_A^i and σ_X^i are compared with data measured previously. Taking into account the combined uncertainties of the results obtained at different laboratories, it is seen that the present cross sections agree for the most part with the earlier data in the region of overlap.

The measurements of x-ray and Auger-electron cross sections can be used to obtain total cross sections σ_K^i for K-shell ionization:

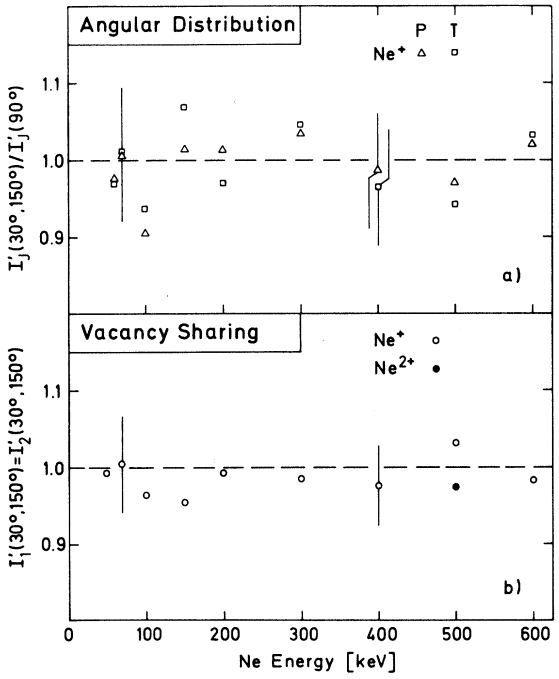

FIG. 6. Angular distribution of Auger electrons and K-shell vacancy sharing between projectile and target atom as a function of the impact energy in Ne^+ (Ne^{2+}) + Ne collisions. Data are from Berlin. (a) The intensity ratio $I_j'(30°,150°)/I_j'(90°)$ of Auger peaks observed at 30°, 150°, and 90°, where $I_i'(30°,150°)=\frac{1}{2}[I_j'(30°)+I_j'(150°)]$. Labels P and T denote the projectile and the target, respectively. (b) The intensity ratio $I_1'(30°, 150°)/I_2'(30°,150°)$ of Auger peaks from the projectile and the target. Peak intensities refer to the rest frame of the corresponding emitter particle.

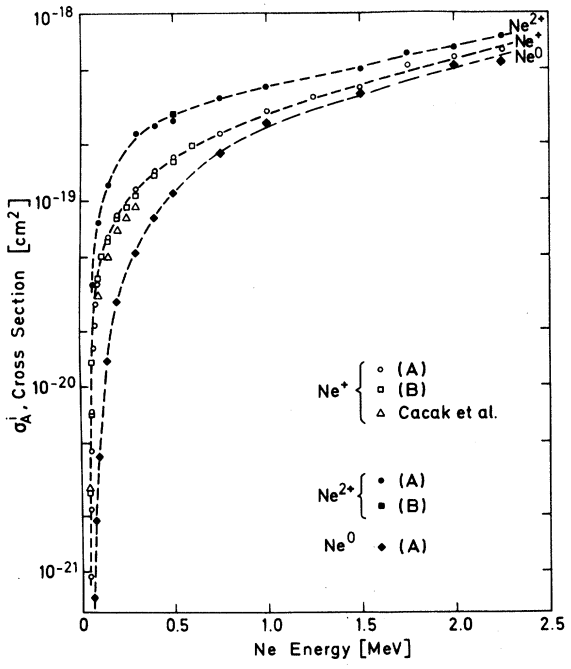

FIG. 7. Total cross section σ_A^i for Auger-electron production in Ne^{i+} + Ne collisions with $i=0$, 1, and 2, as a function of the impact energy. Labels (A) and (B) denote apparatus used in Aarhus and Berlin, respectively. The results by Cacak *et al.* are from Ref. 7.

$$\sigma_K^i = \sigma_X^i + \sigma_A^i \ . \qquad (4)$$

Single x-ray and Auger decay are in first order, the only decay modes for atoms being ionized in the K shell. Thus, we neglect second-order effects such as double-Auger decay which was found to be a contribution of less than 10% for Ne.[40] Figure 9 shows the cross sections σ_K^1, which can be compared with cross sections calculated by Briggs and Macek.[8,41] It should be noted that in the earlier results[8] particle trajectories were calculated using a simple Coulomb scattering potential. Such a potential overestimates the repulsion between the particles; hence these results do not reproduce the threshold behavior of the cross section correctly.[41] In Fig. 9, improved theoretical data are given below 400 keV as calculated more recently by Briggs.[41] The analysis was made with a screened Bohr potential, and using $2p\pi$-$2p\sigma$ energies and coupling appropriate for Ne^+-Ne. Above 400 keV, scaled D^+-D results are given as in the earlier work.[8] (Scaled D^+-D results of Vaaben-Andersen,[42] who performed exact one-electron calculations and also used a screened Bohr potential, agree well with the data of Briggs.) It can be seen that excellent agreement is found between theoretical and experimental results near the K ionization threshold. The theoretical and experimental cross sections begin to disagree above 200 keV, and at 1 MeV the calculated cross sections are a factor of 1.5 lower than the experimental results. The major reason for these discrepancies is that the calculations are based on a two-state theory which is expected to be invalid at high collision velocities,[8] as discussed in Sec. IV E.

E. Exit-channel effect

In the production of a K vacancy, essentially two successive processes are involved. First, an initial $2p$ vacancy may become a molecular $2p\pi$ vacancy; the probability for this to happen is known as the $2p\pi$-vacancy occupation probability. The number of resulting $2p\pi$ vacancies is the $2p\pi$ vacancy-occupation number N_i, where the index i refers to the number of initial $2p$ vacancies, the charge state of the incident particle. The N_i have been calculated by Macek and Briggs[8] to be 0, $\frac{1}{6}$, and $\frac{1}{3}$ for $i = 0$, 1, and 2, respectively. Secondly,

TABLE IV. Cross sections σ_A^0, σ_A^1, and σ_A^2 for Auger-electron production by Ne^0, Ne^+, and Ne^{2+} impact, respectively, and cross section σ_X^1 for x-ray production by Ne^+. Also, $\sigma_X^2 = 91 \times 10^{-22}$ cm^2 and $\sigma_A^2 = 29.5 \times 10^{-20}$ cm^2 were measured at Berlin for 500-keV Ne^{2+} + Ne.

T_0 (keV)	σ_A^0 (10^{-20} cm^2) [a]	σ_A^1 (10^{-20} cm^2) [a]	σ_A^1 (10^{-20} cm^2) [b]	σ_A^2 (10^{-20} cm^2) [a]	σ_X^1 (10^{-22} cm^2) [b]
45	...	0.095	...	...	...
50	...	0.22	0.27	...	0.58
55	...	0.46	...	...	...
60	0.074	0.74	0.74	...	1.67
70	...	...	1.37	...	3.18
75	0.193	1.68	...	3.53	...
80	...	2.16	...	...	...
90	0.437	2.86	...	...	...
100	...	3.69	3.77	7.5	9.1
120	...	...	5.2	...	12.6
150	1.43	6.4	6.3	12.1	15.6
200	2.86	8.3	8.1	...	22.1
250	...	...	9.3	...	24.7
300	5.3	11.0	10.6	22.9	30.3
400	8.3	14.7	13.9	25.1	41
500	11.0	17.1	16.3	27.3	50
600	...	...	19.9	...	62
750	17.9	22.9	...	35.6	...
1000	26.2	30.1	...	41	...
1250	...	36.4	...	...	...
1500	38.5	40	...	51	...
1750	...	53	...	61	...
2000	54	59	...	66	...
2250	55	64	...	76	...

[a] Aarhus.
[b] Berlin.

a rotational coupling, at small internuclear separations, between the almost-degenerate $2p\pi$ and $2p\sigma$ MO's may transfer the $2p\pi$ vacancy down into the $2p\sigma$ MO. This process is characterized by $\sigma_{\rm rot}$, the rotational coupling cross section. The two processes are combined into the following expression for the K-shell ionization cross section:

$$\sigma_K^i = N_i\,\sigma_{\rm rot}\,. \tag{5a}$$

As a result of this description, Ne^{2+}, Ne^{+}, and Ne^{0} impacts on Ne should give ratios of σ_K^i which are 2:1:0, respectively.[3]

The exit-channel effect, well documented at low collision velocities,[5,10] rapidly loses significance with increasing velocity.[11] This breakdown of the exit-channel effect takes place in a well-defined velocity range (0.4–0.7 a.u.) for the first-row atoms,[11] and is explained in the following manner. As the collision velocity is raised, long-range couplings between outer MO's become increasingly important, so that vacancies from empty or partly filled MO's may be transferred into the $2p\pi$ MO with appreciable probability. These dynamic couplings that take place at an early stage of the collision add a velocity-dependent component $N_i(v)$ to the previously defined (static) vacancy-occupation number N_i^0: $N_i = N_i^0 + N_i(v)$, and accordingly, Eq. (5a) must be modified to

$$\sigma_K^i = [N_i^0 + N_i(v)]\,\sigma_{\rm rot}\,. \tag{5b}$$

Here, $N_i(v)$ decreases toward zero for small v, and N_0^0, N_1^0, and N_2^0 are 0, $\frac{1}{6}$, and $\frac{1}{3}$, respectively, as stated above.

From the data in Table IV we derived the ratios $\beta_{1,0} = \sigma_K^1/\sigma_K^0$ and $\beta_{2,1} = \sigma_K^2/\sigma_K^1$. (In this section we set the ionization cross section σ_K^i and the Auger-electron-production cross section σ_A^i to be equal.) The $\beta_{i,j}$ data are shown in Fig. 10. We note that $\beta_{1,0}$ is 10 at 60 keV ($v = 0.346$ a.u.) but drops drastically towards unity as the velocity is raised. At 200 keV it is reduced to 2.9. This value is 70% higher than the earlier result of $1/0.6 = 1.67$ obtained by McCaughey *et al.*[5] At present we are unable to explain this discrepancy, which would appear to be outside the experimental uncertainties. Similarly, the $\beta_{2,1}$ data, which start off at $\beta_{2,1} = 2$ at small velocities, decrease toward unity as the collision velocity is raised.

To evaluate $N_i(v)$ from the experimental data by means of Eq. (5b), we have incorporated theoretical values of $\sigma_{\rm rot}$. The two-state calculations by Briggs[41] and Vaaben-Andersen[42] on σ_K^1 were based on a constant $N_1 = N_1^0 = \frac{1}{6}$, and hence $\sigma_{\rm rot}$ are obtained directly by means of Eq. (5a). The ex-

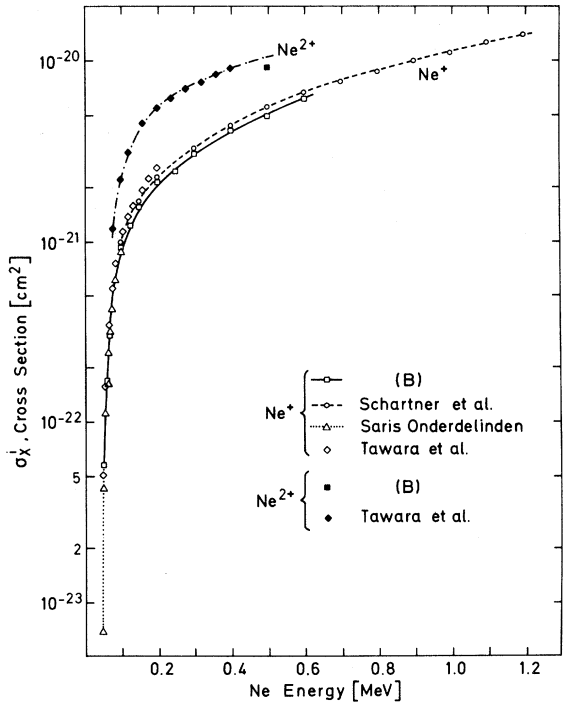

FIG. 8. Total cross section σ_X^i for x-ray production in Ne^{i+} + Ne collisions with $i = 1$ and 2 as a function of the impact energy. Data are from Berlin. The results by Saris and Onderdelinden, Tawara *et al.*, and Schartner *et al.* are from Refs. 16, 17, and 18, respectively.

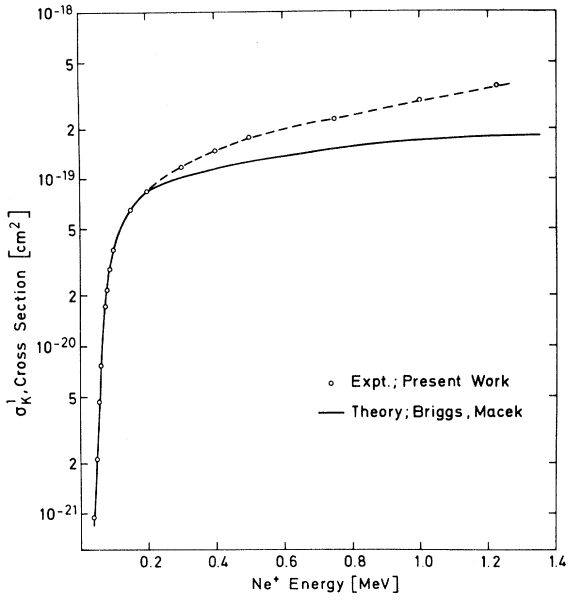

FIG. 9. Total cross section σ_K^1 for inner-shell ionization in Ne^{+} + Ne collisions as a function of incident energy. The experimental results are obtained from $\sigma_K^1 = \sigma_A^1 + \sigma_X^1$, where σ_A^1 was measured at Aarhus and σ_X^1 was taken from Refs. 16 and 18. The data by Briggs and Macek are from Refs. 8 and 41.

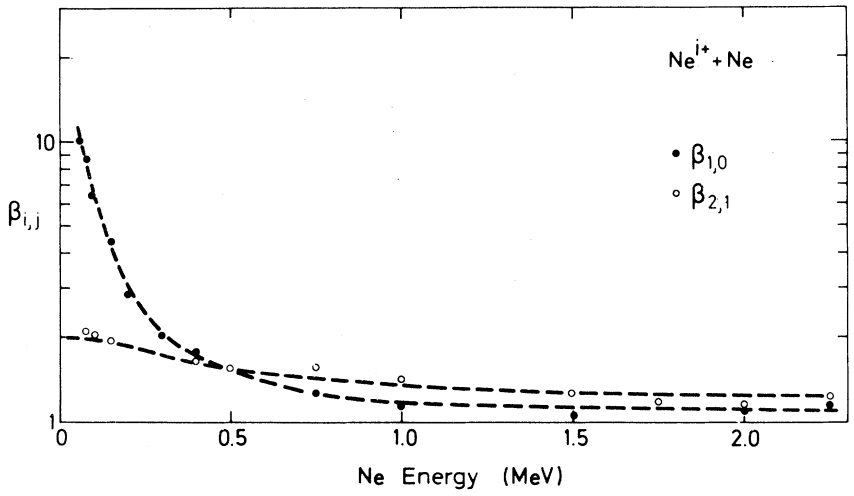

FIG. 10. Cross-section ratio $\beta_{1,0}=\sigma_A^1/\sigma_A^0$ and $\beta_{2,1}=\sigma_A^2/\sigma_A^1$ as a function of incident-particle energy. Data are from Aarhus. σ_A^i denotes the Auger-electron-production cross section for the Ne^{i+} + Ne with $i=0$, 1, and 2, which are here used as approximations to σ_K^i.

cellent agreement between experimental and theoretical σ_K^1 below 200 keV shows that N_1^0 is $\frac{1}{6}$ within a few percent. Further, since $\beta_{2,1}=2$ at low velocities, it also follows that $N_2^0=\frac{1}{3}$ to within a few percent. We notice that these values for N_1^0 comply with a symmetric collision system and that the initial charge state of one of the collision partners does not alter this fact. The surprisingly good agreement between theory and experiment at low velocities makes it tempting to adopt the theoretical σ_{rot} data also at higher velocities. In doing so, however, we should bear in mind that as the velocity is raised, not only is the tail of the rotational-coupling element at larger R becoming increasingly important but also the effective translational factors being used. Hence, the theoretical curve may be less reliable at higher velocities. However, theoretical studies of Vaaben-Andersen,[42] where various reasonable coupling elements and translational factors have been used, suggest that the theoretical data are reliable to within ~10%. Having set the σ_{rot} curve, we can now use Eq. (5b) to derive the dynamic vacancy-occupation number $N_i(v)$ over the measured velocity range, i.e., up to 2.1 a.u. The $N_i(v)$ data have been fitted by a least-squares fit to the following expression as similarly proposed by Barat and Lichten[4] and by Meyerhof[12]:

$$N_i(v)=A_i e^{-c_i/v}. \tag{6}$$

Except at very small v ($v<0.5$ a.u. or $E<125$ keV), the $N_i(v)$ data fit such a relationship very well, as shown in Fig. 11. The constants used in Eq. (6) are $A_0=1.0$, $A_1=1.28$, and $A_2=1.1$, and $c_0=1.85$ a.u., $c_1=3.0$ a.u., and $c_2=3.4$ a.u.

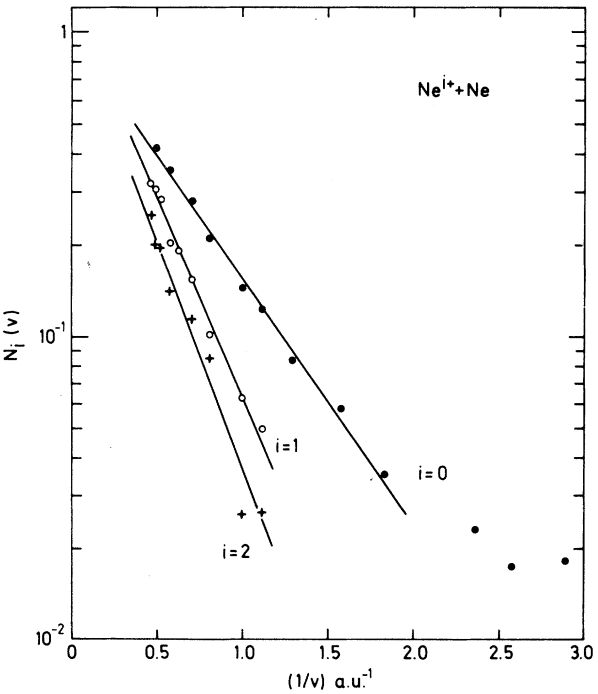

FIG. 11. Vacancy-occupation number $N_i(v)$ ($i=0$, 1, and 2) of the $2p\pi$ MO in Ne^{i+} + Ne collisions vs the inverse projectile velocity. Data are from Aarhus. The solid lines are fits $N_i(v)=A_i e^{-c_i/v}$ with A_i and c_i given in the text.

F. Fluorescence yields

Cross sections for x-ray and Auger-electron production can be used to derive the fluorescence yield averaged over the various states of the excited ion produced in the collision:

$$\bar{\omega}_K^i=\sigma_X^i/(\sigma_X^i+\sigma_A^i), \tag{7}$$

where $\bar{\omega}_K^i$ is the mean fluorescence yield resulting from Ne^{i+}+Ne collisions. In Fig. 12 experimental results are given for $\bar{\omega}_K^1$. The data were obtained from σ_A^1 measured at Aarhus and σ_X^1 reported elsewhere.[16,18] Furthermore, values for $\bar{\omega}_K^1$ were deduced from σ_K^1 and σ_A^1 measured simultaneously at Berlin. In Fig. 12 are also given fluorescence yields for H^+ impact. The uncertainty in the absolute values of the fluorescence yield is about ±25%. The relative error in $\bar{\omega}_K^1$ with respect to a variation of the projectile energy and charge state is about ±15% for the simultaneous measurements of the cross sections. The relative error is expected to be larger than ±15% when cross sections from different laboratories are combined. In particular, systematic errors may be significant at the ionization threshold, since in this region the experimental data are strongly dependent on the energy calibration of the ion accelerator used. Tawara *et al.*[17] combined their results with those of Cacak *et al.*[7] and reported fluorescence yields which are higher by a factor of ~1.7 than the present data for 100- and 200-keV Ne^++Ne. This discrepancy, however, is still within the large uncertainties quoted by Tawara *et al.*[17]

The fluorescence yield for Ne^{2+}+Ne can be obtained by comparing σ_A^2 from Table IV and σ_X^2 reported by Tawara *et al.*[17] It is found that $\bar{\omega}_K^2$ is ~15% higher than $\bar{\omega}_K^1$ at corresponding energies. Since this deviation lies within the experimental uncertainties, we cannot definitely conclude that $\bar{\omega}_K^2$ is higher than $\bar{\omega}_K^1$. The fluorescence yield $\bar{\omega}_K^2 = 0.030$ was measured at Berlin for 500-keV Ne^{2+}, in agreement with $\bar{\omega}_K^1 = 0.029$ for that energy. The difference in the outer-shell charge state produced by Ne^+ and Ne^{2+} is relatively small at energies <500 keV [see Fig. 4(b)], so that no significant deviation between $\bar{\omega}_K^2$ and $\bar{\omega}_K^1$ is expected in the studied energy range.

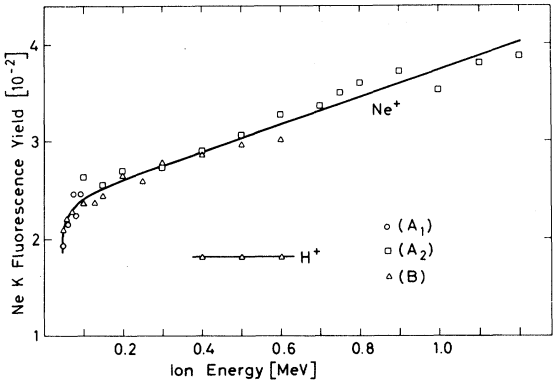

FIG. 12. Mean Ne K-shell fluorescence yield for Ne^+ and H^+ incident on Ne. Data labeled by A_1 and A_2 are a comparison of Auger-production cross sections measured at Aarhus and x-ray production cross sections taken from Refs. 16 and 18, respectively. Label B refers to data measured at Berlin.

Above ~100 keV, the fluorescence yield in Fig. 12 shows a smooth increase with increasing Ne ion energy. This variation is qualitatively understood by the variation of the outer-shell charge state produced. The influence of outer-shell ionization on the fluorescence yield has previously been predicted,[20,21] and recently, fluorescence yields $\omega_K(n)$ for specific vacancy states KL^n have been reported.[25,26,43] The fluorescence yield determined in this study is a mean value $\bar{\omega}_K^1 = \sum_n q_n \omega_K(n)$, where q_n is the probability for producing the KL^n states. This expression can be used to verify the probability q_n by comparing experimental and calculated $\bar{\omega}_K^1$. The probabilities $P_K(n)$ for removal of n L-shell electrons into the continuum are deduced in the Appendix. Moreover, probabilities for production of KL^n states were determined from x-ray spectra,[19] i.e., $\sigma_n^I / \sum_n \sigma_n^I$, in the notation of Ref. 19. The $\sigma_n^I / \sum_n \sigma_n^I$ differ significantly from $P_K(n)$, as demonstrated in Fig. 4(b) by means of the corresponding average numbers $\bar{n}_C$ and $\bar{n}_X$. Above, this was attributed to electron excitation to upper bound states which leaves $\bar{n}_C$ unchanged, whereas it probably increases $\bar{n}_X$. Similarly, we find discrepancies in $\bar{\omega}_K^1$ calculated by replacing q_n by $P_K(n)$ or $\sigma_n^I / \sum_n \sigma_n^I$. As an example, for 400-keV Ne^++Ne, we obtain $\omega_K^1 = 0.021$ and 0.030, respectively, using $\bar{\omega}_K(n)$ by Stolterfoht *et al.*[26] It is seen that the $\bar{\omega}_K^1$ derived from the x-ray data compare well with the present experimental value of $\bar{\omega}_K^1 = 0.029$. This shows that q_n is more adequately represented by $\sigma_n^I / \sum_n \sigma_n^I$ rather than by $P_K(n)$. This in turn suggests that the fluorescence yield is primarily determined by the number of L-shell vacancies and is only weakly dependent on whether the corresponding electrons are removed to upper bound states or into the continuum.

In Fig. 12 the fluorescence yield appears to drop rapidly at the excitation threshold. For 45-keV Ne^+, the fluorescence yield $\bar{\omega}_K^1$ is lower by a factor of ~2 than the corresponding value at 50 keV. A similar variation of the Ne K fluorescence yield has previously been observed by Saris and Onderdelinden[16] and Tawara *et al.*,[17] who both compared cross sections measured at different laboratories. In this case, fluorescence yields determined at threshold are rather uncertain, as mentioned above. Although the results from Berlin for the simultaneous measurement of the cross sections also give slight indication for a possible drop of the fluorescence yield at ionization threshold, it is not certain whether the factor of 2 variations between 45 and 50 keV is a real effect. We suggest

that further measurements of the fluorescence yield are needed near the ionization threshold.

V. COMMENTS AND CONCLUSIONS

In this work, Auger-electron and x-ray production is measured in slow Ne+Ne collisions. Data from two laboratories are combined to give results for various experimental parameters, such as the electron observation angle or energy and the charge-state of the incident ion. The interpretation of the experimental observations is based on the molecular-orbital (MO) model, which is expected to be applicable in the studied energy range. Collision kinematics are studied in some detail to make possible an adequate analysis of the Auger spectra. The data yield results for inner-shell excitation as well as simultaneous ionization of outer-shell electrons. Particular attention is given to outer-shell ionization influencing the production of inner-shell vacancies as well as the subsequent emission of Auger electrons, i.e., K-shell ionization cross section, the mean fluorescence yield, angular distribution of Auger electrons, etc.

Information regarding outer-shell ionization in K-shell ionization collisions are extracted from the centroid energy of the Auger spectra. Here, the major observations are: (a) Various electrons are removed from the L shell during the collision. The mean number of L-shell vacancies observed in the particle with the K-shell vacancy is 2.5 to 3.6 as the Ne^+ energy increases from 100 keV to 2 MeV. (b) The incident charge state of the projectile has no significant influence on the charge state of the collision products. (c) The precollision charge-state difference between target and projectile is not preserved during the collision, i.e., the post-collision charge states are equal for the two particles. Hence, it follows that a certain number of electrons (or vacancies) cannot be specified as belonging to one particle during the collision. This is an observation confirming the molecular nature of the collision, which is the basis for the MO model. (Slight deviations might appear at the high-energy limit of 2 MeV studied here.)

Because of the high degree of outer-shell ionization, the ejection of the K-LL Auger-electrons might not be isotropic. However, such an effect was not observed in the present study. Hence, a possible alignment of the emitter is probably weak due to the averaging effect over the large number of multiplet states produced. To further investigate a possible anisotropy of K-LL electron emission, it is necessary to study specific multiplet states. This may be done by picking out certain satellite lines in higher-resolution spectra, as measured recently.[33,35]

It might be argued that outer-shell ionization influences the K-shell vacancy sharing between the two collision partners. The model by Meyerhof[12] predicts that vacancy sharing is strongly dependent on the K-shell binding energies of both collision partners, which might be altered differently when the collision partners carry different numbers of electrons.[39] Such effects may be expected when the precollision charge-state difference is preserved during the collision. A good indication for this to happen would be that, *on the average,* target and projectile have different post-collision charge states. Indeed, partial preservation of charge-state differences and deviations from equal vacancy sharing have been observed in symmetric high-energy collisions.[37] However, in the present energy range, such effects were not observed.

It might further be argued that, in this work, equal charge states are only observed averaging over several collision products. Singular cases are expected where the post-collision charge states differ significantly and, there, vacancy sharing might not be equal. To verify this possibility, specific coincidence experiments are required; our experimental method does not allow for such a detailed analysis. However, theoretical considerations indicate that such effects are unlikely at lower energies for which the MO model is valid. Formation of specific atomic outer-shell charge states is probably best described by a statistical distribution process. This is expected to take place at large internuclear distances as the particles separate. At intermediate distances, where no specific atomic charge states are formed, the $2p\sigma$ and $1s\sigma$ MO's are probably degenerate; this picture of the collision most likely suggests that K vacancies are equally shared, even when individual charge states of the collision products are quite different. Measurements of post-collisional charge states and K-shell vacancy sharing are expected to be sensitive tests for the breakdown of the MO model at higher energies. We suggest that Ne+Ne collision experiments are required in the energy range of 2–30 MeV.

Outer-shell excitation affects the total cross section for K-shell ionization. These cross sections were found to be in excellent agreement with a two-state rotational-coupling theory at the ionization threshold. However, at higher energies discrepancies appear as additional electrons are removed from the $2p\pi$ MO in the incoming part of the collision. Using the theoretical cross sections from the two-state model, we were able to derive $N_i(v)$, the dynamic vacancy-occupation number, which apparently results from long-range

interactions between outer MO's. Experimentally, we found $N_i(v)$ to obey an expression of the form $N_i(v)=A_i e^{-c_i/v}$, where A_i and c_i depend on the charge state of the incoming particles. By adopting a reasonable model for the creation of $2p\pi$ vacancies due to long-range interactions between outer MO's, one may be able to remove some of the charge-state dependence of A_i and c_i. It has been suggested by Meyerhof that his successful K vacancy-sharing formula may also be applicable to the outer shells.[12] Meyerhof's model predicts an exponential $-1/v$ dependence of the vacancy-occupation probability, in agreement with our empirical formula for $N_i(v)$. However, we expect that the interactions among outer MO's, leading to additional formation of $2p\pi$ vacancies, are far more complicated than anticipated in the Meyerhof model. Hence, we may suggest that the exponential $-1/v$ expression is valid under more general assumptions than incorporated in Meyerhof's model.

ACKNOWLEDGMENTS

We are very much indebted to Dr. P. Dahl for helpful discussions concerning the analysis of kinematic effects and to Dr. J. S. Briggs for communication of his recent calculations.

APPENDIX: THE EXCITATION PROBABILITIES, $P_K(n)$

The probabilities $P_i(m)$ for producing the *final* charge states m of the projectile in Ne^+-Ne collisions have been measured by Fastrup *et al.*[10] The data were obtained for collisions which produce L-shell ionization alone, $i=\mathrm{I}$, and for L-shell ionization plus a single K-shell excitation, $i=\mathrm{II}$. Since the Auger transition, which predominantly (97%) fills the K vacancy, occurs prior to the $P_{\mathrm{II}}(m)$ measurements, and since the K vacancy via the $2p\sigma$-$2p\pi$ coupling ends up in the L shell of either of the collision partners, these distributions $P_i(m)$ do not directly provide the quantities relevant to the x-ray and Auger spectra analysis. Needed, rather, are the probabilities for producing the *initial* defect configuration, where one K vacancy and n L vacancies are excited. In this appendix we show that the probability $P_K(n)$ for removal of one K electron and n L-shell electrons into the continuum can be determined from the $P_i(m)$, providing certain simplifying assumptions about the collision process are made. (We note that in this definition of $P_K(n)$, electrons being excited to upper bound states are not accounted for.) The major assumptions are: (i) The promoted K electron in a collision of type II becomes an L electron of one of the collision partners, and (ii) Apart from process (i), the removal of L-shell electrons and the promotion of the K electron are independent processes. We also neglect the effects of the ~3% x-ray branch, and carry out the analysis only for the projectile; from the symmetry of the collision, the results are equally valid for the K vacancy production in the target recoil.

In a collision of type I no K vacancy is produced, and the defect distribution in outer shells is immediately seen to be given by $P_{\mathrm{I}}(n)$. From this we may easily construct the outer-shell defect distribution $P_K(n)$ for the case where a K vacancy had been produced in the projectile. In doing so, we must, however, bear in mind that the promoted K electron has the probability α to become an L electron in the projectile and thereby reduces the original defect configuration by unity, i.e.,

$$P_K(n)=(1-\alpha)P_{\mathrm{I}}(n)+\alpha P_{\mathrm{I}}(n+1). \tag{A1}$$

Let us now consider a collision of type II, where a K vacancy has been produced with equal probability in either the projectile or the recoil atom. If a K vacancy has been created in the projectile, its outer-shell defect distribution is given before Auger decay by $P_K(n)$. After the Auger process, the outer-shell charge state is increased by 2. One outer-shell electron is emitted and one outer-shell electron has been transfered to the K shell to fill the vacancy there. Since half of the collisions lead to the creation of a K vacancy in the projectile, we have

$$P_{\mathrm{II}}(n+2)=\tfrac{1}{2}P_0(n+2)+\tfrac{1}{2}P_K(n), \tag{A2}$$

where $P_0(n+2)$ is the defect distribution of the projectile in case the K vacancy is produced in the recoil atom. We cannot immediately set $P_0(n+2)$ equal to $P_{\mathrm{I}}(n+2)$, because the K electron promoted from the recoil atom may end up as an L electron in the projectile and thereby reduce the defect configuration by unity. The probability for this to happen is $(1-\alpha)$. Thus, we obtain

$$P_0(n+2)=\alpha P_{\mathrm{I}}(n+2)+(1-\alpha)P_{\mathrm{I}}(n+3). \tag{A3}$$

Substitution of Eq. (A3) into Eq. (A2) yields

$$P_K(n)=2P_{\mathrm{II}}(n+2)-\alpha P_{\mathrm{I}}(n+2)-(1-\alpha)P_{\mathrm{I}}(n+3). \tag{A4}$$

Since at least two outer-shell electrons are involved in an Auger process, it follows that $0\leq n\leq 6$. When $n=6$, the last term in Eq. (A4) vanishes, and $P_{\mathrm{I}}(6)=2P_{\mathrm{II}}(8)-P_{\mathrm{I}}(8)$. The distributions $P_{\mathrm{I}}(m)$ and $P_{\mathrm{II}}(m)$ are both normalized when summed over all m, i.e., $0\leq m\leq 8$. Consequently, $P_K(n)$ derived from either Eq. (A1) or Eq. (A4) are not automatically normalized, and care must be taken with renormalization so that $\sum_n P_K(n)=1$.

We have yet to determine the probability α. Two

limiting possibilities exist here. If the MO correlations are unchanged by the creation of a K vacancy, we expect that the promoted K electron will have equal chances of being attached to the projectile or the recoil atom. This is the same as setting $\alpha = \frac{1}{2}$. If, however, the creation of a K vacancy in one of the collision partners produces an asymmetry in the MO correlations, we may expect that the promoted K electron following the $2p\pi$ MO will go to the partner which has the K vacancy, i.e., $\alpha = 1$. This effect, called "dynamic swapping," was introduced earlier to explain anomalies in the charge-state distributions of asymmetric systems.[1] Therefore, we expect that $0.5 \leq \alpha \leq 1$. To determine α, we combine Eqs. (A1) and (A4), obtaining a relation where $P_K(n)$ is eliminated. The resulting equation can then be solved for α by using the measured $P_i(m)$ data. Such an analysis yields an average value of $\alpha = 0.91$. (For simplicity, we set approximately $\alpha = 1$ in the following.) This means that "dynamic swapping" occurs also in the case of symmetric collisions. Equations (A1) and (A4) now take the form

$$P_K(n) = P_{\mathrm{I}}(n+1) \tag{A5}$$

and

$$P_K(n) = 2P_{\mathrm{II}}(n+2) - P_{\mathrm{I}}(n+2)\ . \tag{A6}$$

It follows directly from these equations that

$$P_{\mathrm{II}}(m+1) = \tfrac{1}{2}P_{\mathrm{I}}(m) + \tfrac{1}{2}P_{\mathrm{I}}(m+1). \tag{A7}$$

TABLE V. Probabilities $P_K(n)$ for simultaneous ionization of one K-shell electron and n outer-shell electrons in 150–400-keV Ne^+ + Ne collisions and mean outer-shell charge state $\bar{n}_C = \sum_n nP_K(n)$. Data are based on results from Ref. 10, see text.

T_0 (keV)	$P_K(n)$ $n=0$	$P_K(n)$ $n=1$	$P_K(n)$ $n=2$	$P_K(n)$ $n=3$	$P_K(n)$ $n=4$	$\bar{n}_C$
150	0.033	0.22	0.53	0.21	0.007	2.01
200	0.031	0.20	0.52	0.24	0.010	2.04
300	0.023	0.175	0.49	0.29	0.024	2.08
400	0.020	0.105	0.47	0.32	0.031	2.19

For the mean charge states we get, correspondingly,

$$\bar{m}_{\mathrm{II}} \simeq \bar{m}_{\mathrm{I}} + \tfrac{1}{2}\ , \tag{A8}$$

where

$$\bar{m}_j = \sum_{n=0}^{8} mP_j(m)\ .$$

From Eqs. (A5) and (A6) follow the approximate formulas for the mean number $\bar{n}_C = \sum_n nP_K(n)$ of outer-shell vacancies produced before Auger decay,

$$\bar{n}_C \simeq \bar{m}_{\mathrm{I}} - 1 \quad \text{and} \quad \bar{n}_C \simeq 2\bar{m}_{\mathrm{II}} - \bar{m}_{\mathrm{I}} - 2\ . \tag{A9}$$

In Table V are given the $P_K(n)$ and $\bar{n}_C$ as obtained by Eqs. (A5), (A6), and (A9) using experimental $P_j(m)$ of Fastrup *et al.*[10] for $T_0\beta_1 = 2000$ keV deg.

*Permanent address: Dept. of Physics, University of Washington, Seattle, Wash. 98195; supported in part by the U. S. Energy Research and Development Administration.

[1]The energy-loss measurements in violent heavy-ion–atom collisions have recently been reviewed by Q. C. Kessel and B. Fastrup, *Case Studies in Atomic Physics*, edited by E. W. McDaniels and M. C. McDowell (North-Holland, Amsterdam, 1973), Vol. 3, p. 137.
[2]U. Fano and W. Lichten, Phys. Rev. Lett. 14, 627 (1965).
[3]W. Lichten, Phys. Rev. 164, 131 (1967).
[4]M. Barat and W. Lichten, Phys. Rev. A 6, 211 (1972).
[5]M. P. McCaughey, E. J. Knystautas, H. C. Hayden, and E. Everhart, Phys. Rev. Lett. 21, 65 (1968).
[6]A recent summary of electron-spectroscopy measurements has been given by M. E. Rudd and J. Macek, in Ref. 1, p. 47.
[7]R. K. Cacak, Q. C. Kessel, and M. E. Rudd, Phys. Rev. A 2, 1327 (1970).
[8]J. S. Briggs and J. Macek, J. Phys. B 5, 579 (1972).
[9]S. Sackmann, H. O. Lutz, and J. Briggs, Phys. Rev. Lett. 32, 805 (1974).
[10]B. Fastrup, G. Hermann, Q. C. Kessel, and A. Crone, Phys. Rev. A 9, 2518 (1974), and unpublished.
[11]B. Fastrup, E. Bøving, G. A. Larsen, and P. Dahl, J. Phys. B 7, L206 (1974).
[12]W. E. Meyerhof, Phys. Rev. Lett. 31, 1341 (1973), and private communication.
[13]N. Stolterfoht, P. Ziem, and D. Ridder, J. Phys. B 7, L409 (1974).
[14]Q. C. Kessel, M. P. McCaughey, and E. Everhart, Phys. Rev. Lett. 16, 1189 (1966).
[15]N. Stolterfoht, D. Schneider, and D. Burch, *Proceedings of the Eighth International Conference on Electronic and Atomic Collisions*, edited by B. Cŏbić and M. V. Kurepa (Institute of Physics, Belgrade, 1973), p. 727.
[16]F. W. Saris and D. Onderdelinden, Physica (Utr.) 49, 441 (1970).
[17]H. Tawara, C. Foster, and F. J. deHeer, Phys. Lett. 43A, 266 (1973).
[18]K. H. Schartner, H. Schäfer, and R. Hippler, Phys. Lett. 46A, 31 (1973).
[19]D. L. Matthews, R. J. Fortner, D. Burch, B. Johnson, C. F. Moore, Phys. Lett. 50A, 441 (1975).
[20]F. P. Larkins, J. Phys. B 4, L29 (1971); 4, 14 (1971).
[21]C. P. Bhalla and M. A. Hein, Phys. Rev. Lett. 30, 39 (1973); and C. P. Bhalla, N. O. Folland, and M. A. Hein, Phys. Rev. A 8, 649 (1973).
[22]D. Burch, W. B. Ingalls, J. S. Risley, and R. Heffner, Phys. Rev. Lett. 29, 1719 (1972).

[23]D. Burch, N. Stolterfoht, D. Schneider, H. Wieman, and J. S. Risley, Phys. Rev. Lett. 32, 1151 (1974).
[24]C. P. Bhalla, D. L. Matthews, and C. F. Moore, Phys. Lett. 46A, 336 (1973); and C. P. Bhalla, *ibid.* 46A, 185 (1973).
[25]D. L. Matthews, B. M. Johnson, L. E. Smith, J. J. Mackey, and C. F. Moore, Phys. Lett. 48A, 93 (1974).
[26]N. Stolterfoht, D. Schneider, P. Richard, and R. L. Kauffman, Phys. Rev. Lett. 33, 1418 (1974).
[27]Preliminary results for the present Ne + Ne fluorescence yields have been reported by N. Stolterfoht, D. Schneider, and D. Burch, *Proceedings of the Fourth International Conference on Atomic Physics*, edited by J. Kowalski and H. G. Weber (Heidelberg, 1974), p. 643.
[28]M. E. Rudd, B. Fastrup, P. Dahl, and F. D. Schowengerdt, Phys. Rev. A 8, 220 (1973).
[29]B. Fastrup, G. Hermann, and K. J. Smith, Phys. Rev. A 3, 1591 (1971).
[30]N. Stolterfoht, Z. Phys. 248, 81 (1971).
[31]N. Stolterfoht, D. Schneider, and P. Ziem, Phys. Rev. A 10, 81 (1974).
[32]G. N. Ogurtsov, I. P. Flaks, and S. V. Avakyan, Zh. Eksp. Teor. Fiz. 40, 2124 [Sov. Phys.—JETP 15, 1656 (1971)].
[33]D. Burch, N. Stolterfoht, D. Schneider, H. Wieman, and J. S. Risley, University of Washington, Nuclear Physics Laboratory Annual Report 1974 (unpublished), p. 167.
[34]N. Stolterfoht, H. Gabler, and U. Leithäuser, Phys. Lett. 45A, 351 (1973).
[35]D. L. Matthews, B. M. Johnson, J. J. Mackey, and C. F. Moore, Phys. Rev. Lett. 31, 1331 (1973); and D. L. Matthews, B. M. Johnson, J. J. Mackey, L. E. Smith, W. Hodge, and C. F. Moore, Phys. Rev. A 10, 1177 (1974).
[36]M. O. Krause, T. A. Carlson, and W. E. Moddeman, J. Phys. (Paris) 32, C4-139 (1971).
[37]N. Stolterfoht, D. Schneider, D. Burch, W. Wieman, and J. S. Risley, Phys. Rev. Lett. 33, 59 (1974). Note that the projectile cross sections presented in Table I of this reference are in error and should be divided by two.
[38]W. Mehlhorn, Phys. Lett. 26A, 166 (1968); and B. Cleff and W. Mehlhorn, J. Phys. B 7, 593 (1974).
[39]J. Eichler and U. Wille, Phys. Rev. Lett. 33, 56 (1974); and J. Eichler and U. Wille, Phys. Rev. A 11, 1973 (1975).
[40]T. A. Carlson and M. O. Krause, Phys. Rev. Lett. 14, 390 (1965).
[41]J. S. Briggs, *Proceedings of the International Conference on Inner-Shell Ionization Phenomena,* edited by R. W. Fink, S. T. Manson, I. M. Palms, and P. V. Rao (U. S. AEC, Oak Ridge, Tenn., 1973), p. 1209; and private communication.
[42]J. Vaaben-Andersen (private communication, 1975).
[43]M. H. Chen, B. Crasemann, and D. L. Matthews, Phys. Rev. Lett. 34, 1309 (1975).